Landslides
DOI 10.1007/s10346-017-0942-4
Received: 13 June 2017
Accepted: 28 December 2017

M. Medjkane · O. Maquaire · S. Costa · Th. Roulland · P. Letortu · C. Fauchard · R. Antoine · R. Davidson

High-resolution monitoring of complex coastal morphology changes: cross-efficiency of SfM and TLS-based survey (Vaches-Noires cliffs, Normandy, France)

Abstract High-resolution digital elevation models (HRDEMs) on coastal areas, particularly cliffs, are an important asset for analyzing and quantifying the processes affecting their morphology. The Vaches-Noires coastal cliffs, located at the north-western part of the Pays-d'Auge region (Normandy, France), are an ideal site for the study of subaerial and marine erosion processes. Indeed, the coastline evolves through the accumulation of deposits resulting from rotational landslides and/or mudflows at the base of the cliff which are then undermined by the sea. The 3D modeling of a representative sector of the cliffs appears a suitable solution to monitor and quantify this evolution using HRDEMs. This paper presents the whole of a monitoring protocol, with high spatial resolution and high temporal resolution, on an original location characterized by reliefs of Badlands in coastal environments. The first results of these investigations are described with an evaluation of two methods for the creation of 3D models: a "heavy" method by Terrestrial Laser Scanning (TLS) monitoring, and a "light" method using "Structure from Motion" (SfM) terrestrial photogrammetry. The small investment of time in the field and money is an important asset of the SfM method. The textured rendering quality of the SfM model makes it a powerful tool for geomorphological analysis. According to a recurrent monitoring protocol involving both measurements, it was possible to compare the accuracy of the SfM and TLS models. The results show a high accuracy of the SfM models with an overall average error of 0.05 m. The representations of the zones of accumulation and erosion as well as their spatial succession allow to investigate the dynamics of the involved processes with both methods. Preliminary volume calculation results are conclusive for TLS models.

Keywords Structure-from-motion · Terrestrial laser scanning · Coastal processes · Coastal morphology · Landslides · Mudflows

Introduction

The high-resolution modeling of coastal areas and the precise measurement of their evolution over time contribute to a better understanding of the dynamic processes which generate these morphologies. In this context, the creation of high resolution digital elevation models (HRDEMs) has become an important issue in particular in the investigation of landslide problems (Jaboyedoff et al. 2012; Sofia et al. 2016).

Nowadays, the fast development of active and passive close-range sensing techniques allows high spatial and temporal resolution tracking of landforms. Two techniques are particularly suitable for their ability to measure in three dimensions and high resolution the earth's surface: laser scanner and photogrammetry (Abellán et al. 2016).

LiDAR (light detection and ranging) is an active remote sensing technique mainly used to create high-resolution models with high accurate representation of a dense 3D point cloud. The final quality of the HRDEMs resulting from LiDAR technique depends to a large extent on the relative distance of the studied object from the measurement point: from decimeter resolutions for airborne laser scanners (ALS) (Harwin and Lucieer 2012; Ruggles et al. 2016) to millimeter resolutions for terrestrial laser scanner (TLS) (Jaboyedoff et al. 2012; Eltner and Baumgart 2015).

In the past few years, photogrammetry techniques have undergone a major revival thanks to developments in the field of computer vision, especially the generation of 3D surface models with the structure from motion (SfM) approach for a spatial point cloud reconstruction (Lowe 1999; Lowe 2004) and democratization of ergonomic computer tools for the non-specialist user (Abellán et al. 2016; Westoby et al. 2012; Smith et al. 2015; Michelletti et al. 2015). Like the TLS, the final resolution of SfM models is strongly dependent on the scale of analysis of the object studied and its distance from the measurement points. Nevertheless, several studies have confirmed the quality of the resolution of the HRDEMs produced by SfM up to a decimeter precision or even lower in the most optimal cases (Smith et al. 2015; Favalli et al. 2012; James and Robson 2012).

TLS produces, at comparable distance of acquisition, the most accurate measurements with nevertheless the disadvantages of high costs and the requirement of a strong material and time investment which may be incompatible regarding the accessibility of certain study sites (Roer and Nyenhuis 2007; Piermattei et al. 2016; Letortu et al. 2015). In contrast, structure-from-motion techniques require little investment in both money and time of acquisition in the field, thus constituting a reactive and inexpensive observation method (Eltner et al. 2016; Michelletti et al. 2015).

The modeling approach resulting from these 3D acquisition techniques is now more and more widespread in the field of geosciences. There are applications in the field of soil study (Castillo et al. 2012; Stöcker et al. 2015; Nouwakpo et al. 2015), the study of glacial and periglacial zones (Piermattei et al. 2016; Nolan et al. 2015; Rippin et al. 2015; Immerzeel et al. 2014), fluvial geomorphology (Dietrich 2016; Woodget et al. 2015; Prosdocimi et al. 2015), and volcanology (Slatcher et al. 2015; James and Robson 2012; Bretar et al. 2013). Landslides studies (Stumpf et al. 2014; Jaboyedoff et al. 2012; Teza et al. 2007; Lucieer et al. 2013) and coastal geomorphology (Mancini et al. 2013; Ružić et al. 2014; James and Quinton 2014) are also investigated to a minor extent (Jaboyedoff et al. 2012; Eltner et al. 2016).

The work presented here shows an example of application of these methods of 3D acquisition on coastal sites whose morphology makes the fine modeling of the areas difficult. The study gives an account of the empirical investigations

Published online: 25 January 2018

carried out since September 2014 on the Vaches-Noires cliffs in Villers-sur-Mer, Normandie, France, thanks to the cross-efficiency of the TLS and SfM measurements for high-resolution, spatio-temporal monitoring of the slope and coastline dynamics. Research carried out on these Vaches-Noires cliffs has four mains objectives: (1°) to define velocities and rhythms of slope evolution by the different processes (areolar and particular erosion, slides, mudflows,…); (2°) to determine volumes of ablation and accumulation of materials seasonally and annually; (3°) to evaluate the evolution of the coastline (basal scarp); (4°) to determine agents and factors responsible for these processes.

After a description of the geomorphological characteristics of the study site, a spatio-temporal tracking protocol using 3D modeling is presented. The results are then discussed in terms of evaluation of the microtopography of the site and comparison of the SfM and TLS renderings. Finally, the perspectives offered by this investigation protocol are set out.

Study site

In Normandy (France), between Houlgate and Villers-sur-Mer, the cliffs of Vaches-Noires extend for nearly 4.5 km. These cliffs have a complex and chaotic morphology, evolving under the action of continental and marine subaerial processes.

The "Pays d'Auge" plateau which reaches a maximum height of 120 m a.s.l is limited by a main scarp (Fig. 1). This 10–20-m high scarp runs parallel to the coastline and shows large concavities. It is followed by a bench with a bumpy and chaotic morphology limited by a secondary scarp. Armed with Jurassic limestone (from 10 to 15 m high), this scarp evolves and retreats in rotational slides (Fig. 2). At the bottom part, in the Jurassic marly formations, interfluve crests (C) crop out generally perpendicular to the coastline. They separate deep thalwegs (G) where mudflows (F) are more or less active. The morphology of theses flows is characterized by lobes corresponding to different phases of successive activities.

Interfluve crests and talweg flanks are also affected by particle detachment, diffuse gullying processes (superficial weathering), and small superficial slides (Fig. 2): basal scarps ("active" cliff smaller than 5 m), alternating periods of accumulation (supply of materials from the upper part by mudflows) and periods of erosion when the sea undermines the basal scarp. In the axis of gullies, blocks of multi-meter dimensions, transported by the flows, arm and locally protect the foot of the cliff or get stuck on the foreshore (Maquaire et al. 2013; Auger and Mary 1968; Maquaire and Malet 2006).

In response to the objectives presented in the first section, a diachronic monitoring coupled with 3D modeling using TLS and SfM was committed as part of the SNO DYNALIT (National Observation Service focused on the study of coastal and coastline dynamics) on an easily accessible site, except in periods of high tides, immediately located to the western part of Villers-sur-Mer. This site was chosen due to its representative dynamics of the Vaches-Noires cliffs and the availability of some fixed landmarks such as the coastal dike protection and the "ruined" building at the top of the cliff (Fig. 4). The observation site (about 200 m wide) thus comprises six thalwegs (Go to G6) associated with flows (Fig. 4). The monitoring process focuses on the three thalwegs (G3 to G5) and associated "active" mudflows (F2 and F3) located in the central part of the constructed 3D model.

Material and methods

General framework

Measurements and 3D modeling of the study site have been carried out since September 2014 using a single protocol combining laser scanning and photographic survey (Fig. 3). The dates enclosed in red dashes in Fig. 4 represent the measurements taken into account for the SfM/TLS comparison in this paper. In addition to the objective of microtopography diachronic monitoring of the Vaches-Noires cliffs, the aim is to compare the quality of the SfM renderings with respect to the TLS models which are, in this context, the reference models (Smith et al. 2015; Smith and Vericat 2015; Westoby et al. 2012; Kaiser et al. 2014; Chiabrando et al. 2014; Eltner et al. 2015). Indeed, the calibration of these SfM methods still requires setting up a protocol for cross-checking the relevance of models produced by terrestrial photogrammetry (Eltner et al. 2016; Abellán et al. 2016).

The observation campaigns of the Vaches-Noires site followed this cross-checking protocol which aims to validate the relevance of the models with the implementation of quasi-systematic cross-measurements by TLS and terrestrial photogrammetry. Local weather conditions (rainfall) may make some of the field measurements difficult on certain dates. The resulting models are georeferenced from ground control points (GCPs) as seen in Fig. 5.

The coordinates of these GCPs are defined at ± 1 cm accuracy with total station measurements based on a fixed base canvas determined by Differential GPS (DGPS Trimble with a base station 5700 and a mobile receiver R6). The total station, whose calibration point is precisely measured by DGPS, allows the local coordinate system of the SfM and TLS points clouds to be transformed to a global coordinate system (RGF93-Lambert93: EPSG: 2154)(Letortu et al. 2015). The offset of the different reflectors (total station, TLS, SfM) has been taken into account when measuring these coordinates. The following figure (Fig. 4) shows the general scheme of the various measurements and the position of the GCPs.

Terrestrial laser scanner

The eight laser surveys at the Vaches-Noires site are based on a full-waveform RIEGL VZ400 terrestrial laser scanner with a theoretical range of 400 m. The instrumental accuracy of the TLS is ±0,003 m for 50 m. The angular resolution was set to 0.02°, allowing a fine scan of the slope in less than 5 min (horizontal window of 130° and vertical of 30°). Several scans are carried out at each survey from three stations (Scan 1 to Scan 3) about 50 m from the coastline (Fig. 5) and from a fourth station (Scan 4), located at the lower part of the slope. These four stations have partly resolved the classical occlusion problem, caused by topography and vegetation. DEM modeling resulting from the TLS survey requires several stages of 3D data processing: multi-scan adjustment and georeferencing; 3D point cloud cleaning; triangulation (mesh) and HRDEM creation.

The scanning of each position is recorded as a 3D point cloud (x,y,z) in a reference system relative to each position of

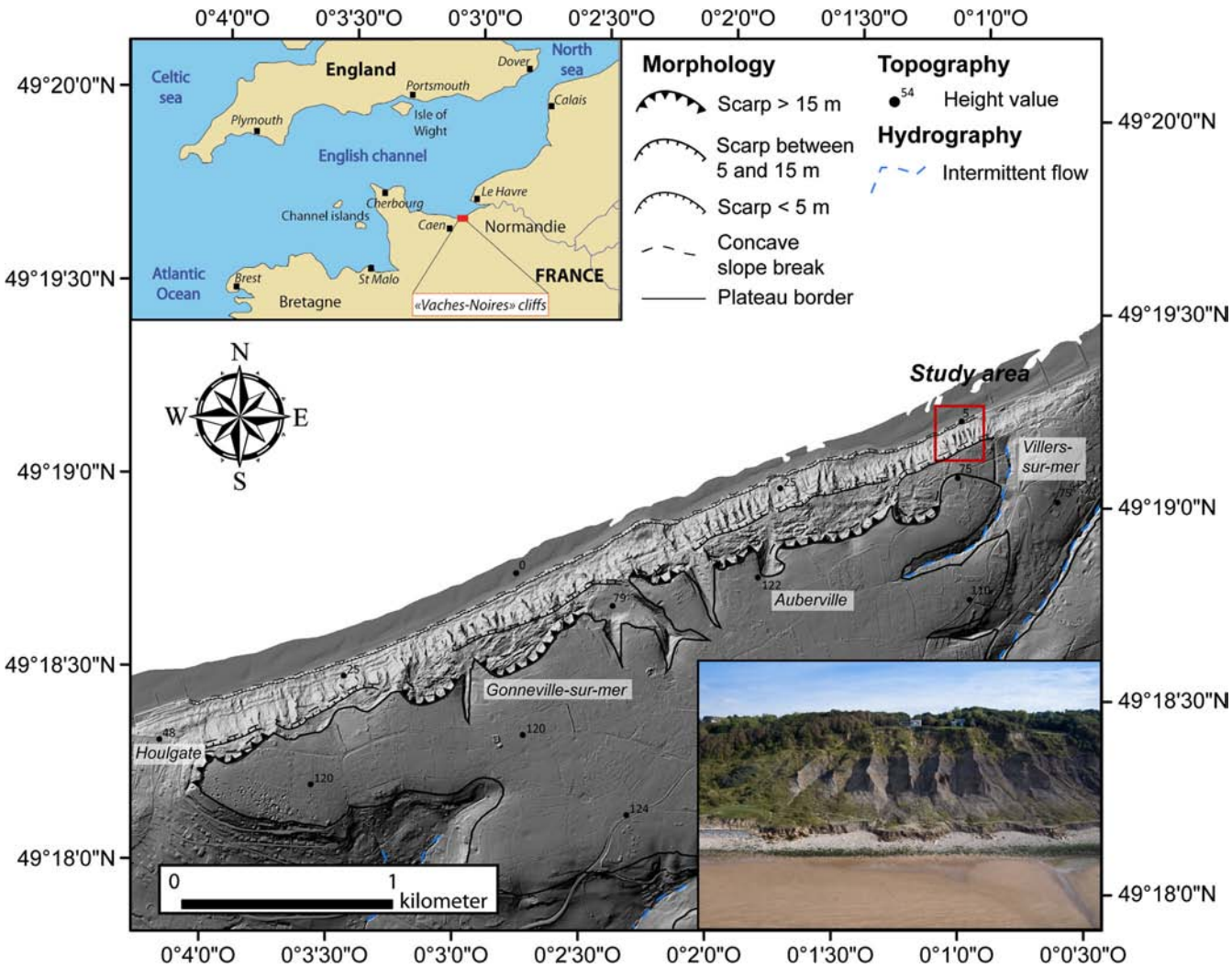

Fig. 1 Study area in Normandy (France): location and simplified morphological map of the Vaches-Noires cliffs and scarps (source: Litto 3D Digital Terrain Model, IGN)

the scanner in the field: the multi-scan adjustment consists of the integration of the different scans into a common reference system. This adjustment is obtained by using the georeferencing targets evenly distributed over the study area (Fig. 5). The *Iterative Closest Point* algorithm (*ICP*, (Prokop and Panholzer 2009)) is used to fit each scan in the same spatial reference. The precision of the fit is determined by comparing the accuracy of control points on the model with the precisely measured GCPs by calculating the RMSE (*Root Mean Square Error*, (Eltner et al. 2016; Kaiser et al. 2014)).

Post-processing was carried out using the Riscan Pro 2.0 software: all laser measurements were reduced, in order to distinguish only a maximum of four echoes (Jaboyedoff et al. 2012; Shan and Toth 2008; Prokop and Panholzer 2009) from which it is possible to identify and eliminate the first, last and intermediate echoes (e.g. vegetation elements). Then, by iteration and manual cleaning, the artifacts of the measurements (reflections, false measurements below or above the ground) and the rest of the vegetation are eliminated in order to keep only the characteristics of the ground morphology (Travelletti et al. 2013; Letortu et al. 2015). The final DEM is obtained by triangulation/rasterization ("mesh") of the TLS 3D point cloud: a choice of resolution adapted to the characterization of the site's microtopography is determined to degrade the expected millimeter accuracy of the measurement to sufficient centimeter accuracy.

Terrestrial photogrammetry

The so-called "*Structure from Motion*" photogrammetry method is based on mathematical principles of 3D reconstruction using 2D information, such as photographs, using a "Scale Invariant Feature Transform" algorithm, (SIFT, (Lowe 1999; Lowe 2004)). Like TLS, the result of the SfM approach is a 3D point cloud.

The model generation followed the method presented in Eltner et al. (2016) on SfM processing steps: object recognition, image matching and orientation of camera (*feature detection/image matching*); camera alignment optimization; densification of the 3D point cloud (*dense matching*); triangulation / rasterization (*meshing*) and finally texturing (*rendering*) of the model. Agisoft Photoscan software has been chosen for its qualities of 3D reconstruction of complex environments (Chiabrando et al. 2014; Kaiser et al. 2014) and ergonomics

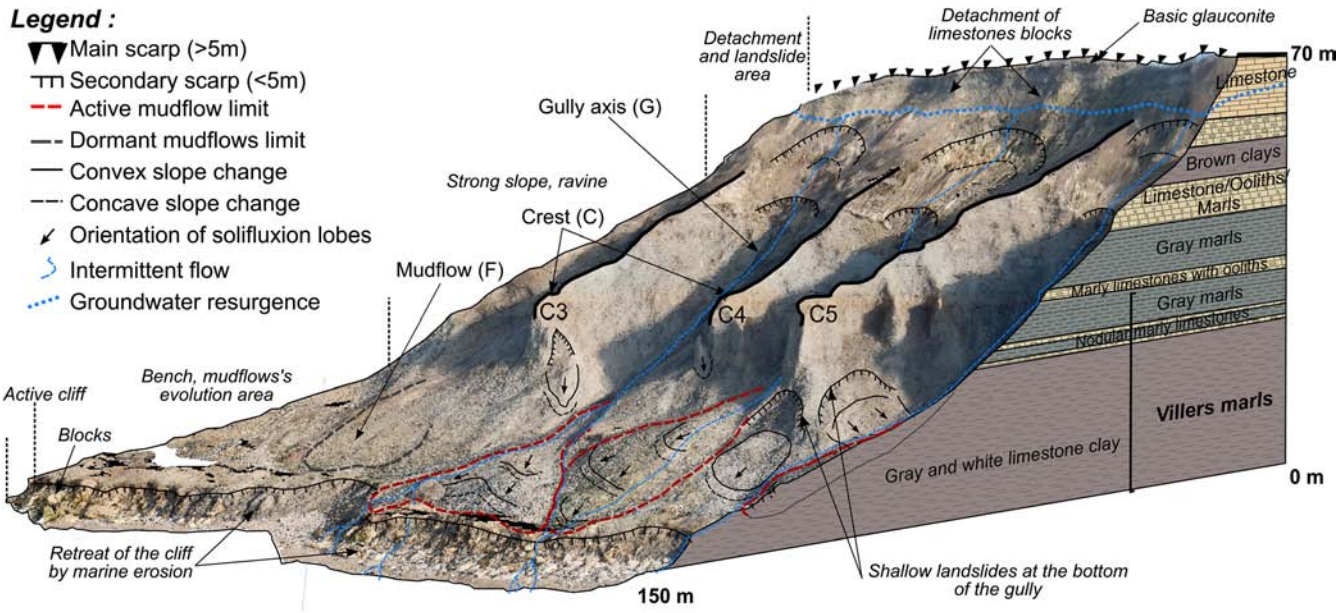

Fig. 2 Interpretative block diagram of processes affecting the Vaches-Noires cliffs and scarp (Thomas, 2015)

of use allowing automation of the procedure (Eltner et al. 2016). The final resolution of the generated model depends on the relative distance of the camera position to the object. The overlap, coverage, and image sharpness determine the success of the image matching routine. Although the first points have been extensively commented (e.g. Eltner et al. 2016; Kaiser et al. 2014; Westoby et al. 2012), one seldom finds a clear methodology in scientific literature that explains how to shoot quality images (James and Robson 2014; Tournadre et al. 2015).

First, the camera has to be efficient, i.e., with a sufficient number of pixels and quality optics. Over the site of the Vaches-Noires, the photographs were initially taken with a Nikon Coolpix S9700 (16 million pixels; sensor size 6.17 × 4.55 mm; focal length 25 mm). This consumer grade camera allowed to test the first models of the site for the measurements of March, June and September 2015. Thereafter, an investment in a more advanced grade camera has allowed to refine the accuracy of measurements from February 2016 with a Nikon D810 (36 million pixels; sensor size 36 × 24 mm) and a Sigma 35 mm fixed optics. The quality of this gear provides dense measurements (high number of pixels) *which are* directly correlated with the quality of the model produced during the dense matching stage (Clapuyt et al. 2016). Furthermore, the Sigma fixed optics was chosen for its photographic reproduction qualities with minimal distortion.

The shooting parameters in the field were then adjusted according to the scene illumination context. In order to maintain maximum sharpness in all areas of photography, it is necessary to keep a low sensitivity (ISO) parameter and a high Depth of Field (f/stop) parameter. The surveys were carried out with an ISO '100' and a depth of field of 'f / 16'. The opening time of the diaphragm is then adjusted according to the local illumination conditions, which sometimes requires the use of a tripod to avoid motion-blur.

In addition, the raw file format of the photographs (*.raw format) has been chosen, because it allows in a post-processing step the precise adjustment of shooting parameters, if necessary. However, the time taken for ground-based shot may imply sudden changes in illumination conditions and shadows on the ground. This is why the photographs were post-processed with the software "LightRoom CC" (Adobe), in order to obtain an overall improvement in the sharpness of the photographs as well as a harmonization of the photographs' quality.

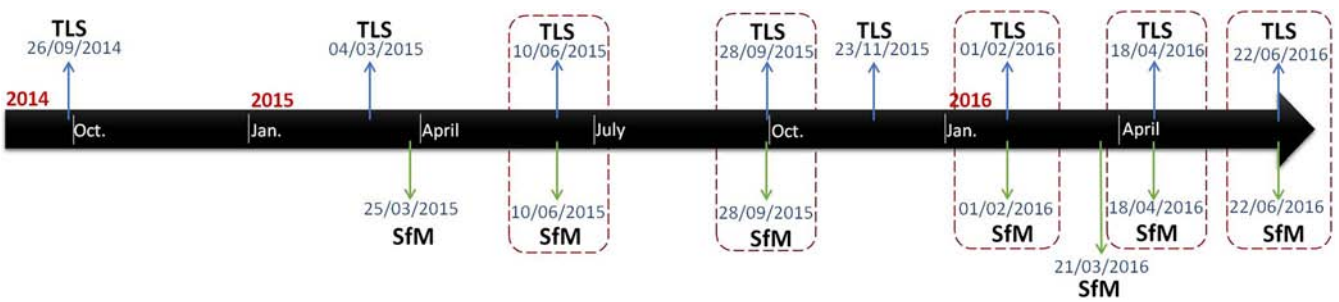

Fig. 3 Dates of the SfM/TLS measurements campaigns on the Vaches-Noires cliffs, Villers-sur-Mer

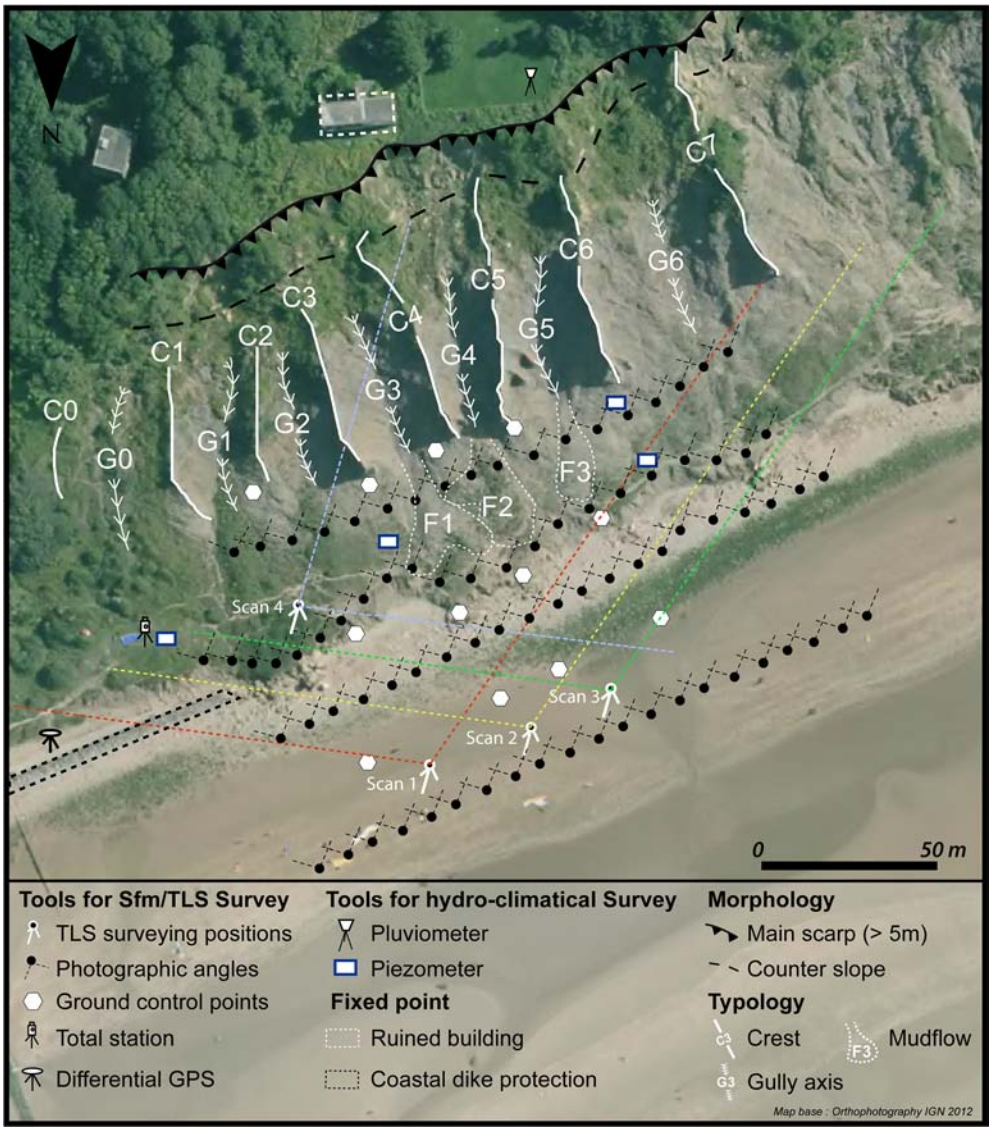

Fig. 4 Measurement scheme of the different points of view and results from the geomorphological/geological landslide mapping

Finally, several experiments were conducted in terms of shots. For proper reconstruction of the model and in order to be able to efficiently process the whole study area, it is necessary (1) to have an important overlap (at least 80% both in width and height) between the photographs, (2) to multiply as much as possible the number of the latter, and (3) to do shots at several distances of the targets. However, the computation time increases with the number of processed images (Eltner et al. 2016). Therefore, according to each area of interest, it is necessary to adjust the number and the coverage of the photographs in order to obtain a fine model of the zone while keeping a reasonable calculation time.

Several tests were carried out on the method of shooting in the field. Models produced with one or two shooting lines only have very low resolution on the top of the slope. Divergent shots (i.e., several photos taken from the same point but with a different horizontal angle) on several lines generated very large reconstruction errors, sometimes going as far as the impossibility of determining a valid solution of *homologous* tie-points. It has been found that three or four shooting lines in a generally similar orientation are the best compromise for both allowing sufficient overlap between photographs and at the same time allowing the entire study scene to be scanned with optimum resolution from the beach to the top of the slope.

The georeferencing targets (GCPs; Fig. 5) used for the calibration of the TLS models are used here for the adjustment of the SfM models on the same reference frame. This georeferencing stage has been conducted after the alignment process and before the optimization and dense reconstruction stage. It has been demonstrated (Tahar 2013) that 6 to 8 GCPs distributed evenly over the area to be modeled is necessary to allow good accuracy of georeferencing. We used 12 GCPs distributed in the field (Fig. 4) and made up of reflective targets for the georeferencing of the TLS measurements and graphic targets for the SfM ones.

The RMSE method is also used to assess the accuracy of HRDEMs from photogrammetric models. Finally, the calibration parameters of the Nikon D810 camera have been integrated with

Fig. 5 Setup of the used Ground control point to georeference both the SfM and TLS models

the "Agisoft Lens" software, in order to improve the efficiency of the SfM reconstruction algorithm.

The comparison between TLS and SfM HRDEMs is carried out using the DEM of Difference (DoD): 3D point clouds are gridded (grid resolution: 5 cm) to generate DEMs which are then differentiated on a pixel-by-pixel basis using ArcGIS 10.4 (ESRI). Unlike some coastal site of sub-vertical cliffs, the Vaches-Noires cliffs are of little steep slopes, so the DoD method can in this case be justified. Thus the altitude variations between two models can be assessed (Wheaton et al. 2009; Schürch et al. 2011).

The calculation of the eroded and accumulated volumes was achieved using the differential models obtained. This calculation includes the areas of interest, the ablation zone, and the accumulation zone, which have been manually identified according to the processes and associated morphologies. At this stage, a simple GIS method (Geographical Information System, ArcGis 10.4, Esri) consisting of the delimitation of cubes whose size is derived from the length and width of the reference pixel (5×5 cm) and the height expressed by the altitudinal differences estimated. Low erosion/accumulation values below the model margin of error are not taken into account.

The following diagram shows the general processing plan of the TLS and SfM measurements (Fig. 6).

Results and discussion

The models produced between September 2014 and June 2016 allow both to evaluate the relevance of the SfM method in comparison with the TLS surveys and to have initial elements concerning the dynamics of the coastal morphology of the Vaches-Noires site (Fig. 7).

Comparison SfM versus TLS

For each date, HRDEMs derived from the 3D point clouds of the TLS and SfM measurements are compared with each other in order to highlight the relative modeling errors of the SfM method.

There is a very high quality and consistency in the measurement accuracy of the TLS with RMSE ≤ 1 cm (Table 1). The SfM models have gradually increased in accuracy after the better camera was used (RMSE between 2.9 and 5.78 cm). Nevertheless, the models still suffer from the effects of the terrestrial shots which generate "shadow zones" due to the chaotic topography of the site. In the case of SfM models, the consequence is the presence of holes in the model. For TLS models this is less obvious, although in these areas, the quality of the modeling can be reduced because of a less efficient interpolation at these sites during the triangulation/rasterization stage. The precision retained in the models was degraded at a resolution higher than the RMSE error observed at each date, thus preventing possible statistical biases. Over the whole period, the TLS models have an accuracy of ± 3 cm, and the SfM models from ± 3 to ± 6 cm, with the exception of the surveys carried out with the Nikon Coolpix, due to a lower sensor size than the D810 camera. Thus, the surveys of 03/25/2015 and 09/28/2015 obtain an accuracy of ± 15 and ± 9 cm. A much larger number of shots during the survey of 06/10/2015 (437 photos) allowed to put into perspectives this weakness, with a final accuracy of ± 5 cm.

One the one hand, the comparison of the TLS and SfM models from June 2015 leads to an average altitude difference of the SfM model between 20 and 50 cm (Fig. 8), but this error includes strong distortions in vegetated areas, "shadow zones" (± 1 m) and the borders of the study area (± 3 m).

On the other hand, the central zone, corresponding to the gullies from G3 to G5, and for which the best accuracy were expected, presents a weak error of ± 10 cm. This is consistent with the expected margins of error when comparing two models with an accuracy of ± 5 cm (Clapuyt et al. 2016).

The models derived from SfM show their efficiency and relevance with high spatial resolutions approaching the precision of the laser scanner to ± 10 cm.

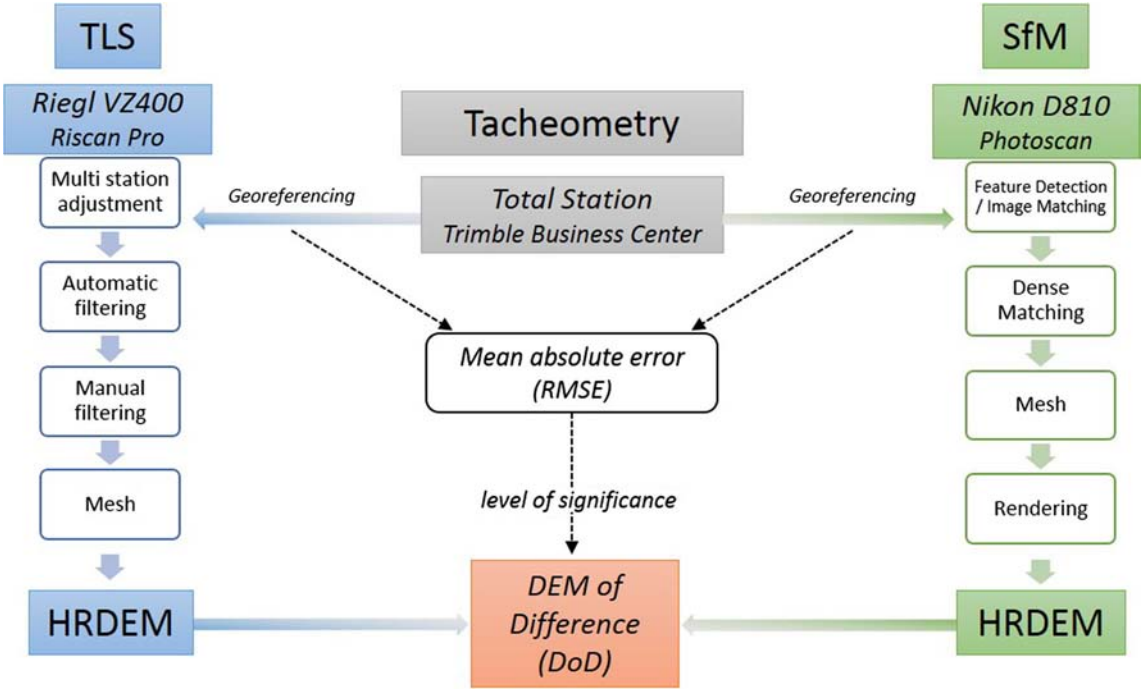

Fig. 6 TLS and SfM processing plans

It should also be noted that the process that contributes to modeling SfM is much more efficient in rendering textured models than in the case of a TLS model.

When scanning a site, the TLS takes only two or three photographs depending on the horizontal angle chosen to scan the study area. This is not enough to create a textured model

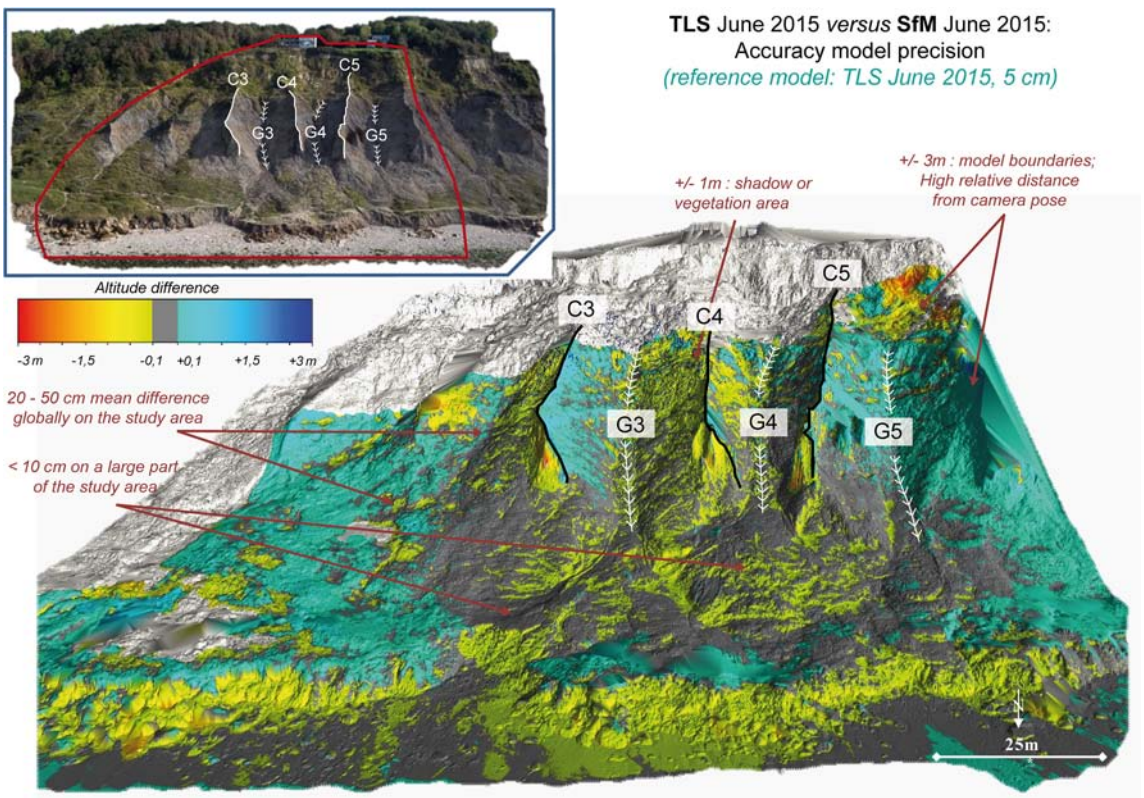

Fig. 7 Comparison of TLS and SfM models with respect to the altitudinal differences between the models calculated by DoD, 06/10/2015

Table 1 SfM and TLS models: summary statistics

	Scans/Photos count		Georeferencing error RMSE		Point density		Final model resolution (cm/pix)	
Date	TLS (scan)	SfM (photos)	TLS	SfM	TLS	SfM	TLS	SfM
26/09/2014	3		1,15 cm		1500 pts/m²		3 cm	
04/03/2015	3		0,94 cm		1500 pts/m²		3 cm	
25/03/2015		175 (Coolpix)		14,17 cm		208 pts/m²		15 cm
10/06/2015	3	437 (Coolpix)	1,06 cm	4,46 cm	4600 pts/m²	1854 pts/m²	3 cm	5 cm
28/09/2015	3	267 (Coolpix)	0,99 cm	8,27 cm	5000 pts/m²	875 pts/m²	3 cm	9 cm
23/11/2015	4		1,08 cm		7000 pts/m²		3 cm	
01/02/2016	4	257 (D810)	1,27 cm	4,19 cm	5900 pts/m²	2100 pts/m²	3 cm	5 cm
21/03/2016		371 (D810)		2,90 cm		784 pts/m²		3 cm
18/04/2016	4	276 (D810)	1,03 cm	5,78 cm	7500 pts/m²	586 pts/m²	3 cm	6 cm
22/06/2016	3	606 (D810)	1,16 cm	3,80 cm	4500 pts/m²	1400 pts/m²	3 cm	4 cm

from all angles. In contrast, the process of Structure-from-Motion involves the use of hundreds of high resolution photographs from different angles, thus enabling the algorithm to choose perfectly the relevant photographs to texture each parcel of the model. It then constitutes an important asset for morphological analysis and interpretation of landscapes for the geomorphologist as shown in Fig. 8 and Fig. 7.

Detection and quantification of active zones by a diachronic approach

The SfM and TLS technique, the adopted methodology and the obtained inherent accuracy allow to locate and quantify the evolutions of the studied badlands. Thus, it is possible to identify the hydro-gravitational processes on the slopes and their links in time and location.

This can be illustrated by the TLS differential models (Fig. 9a) and the SfM differential models (Fig. 9b) obtained on the first of February 2016 and the 22nd of June 2016. First, it can be seen clearly that different surfaces are in good agreement between the two models and methodologies (margin of error = ± 3 cm for the TLS, ± 5 cm for the SfM), except on the edges of the SfM and TLS model with a decrease in resolution and accuracy which leads to some modeling artifacts (e.g., the top of the cliff above crest C5 and C6 or the eastern part of the SfM model).

As demonstrated, the main sectors of erosion and accumulation are well demonstrated on the TLS and SfM models with a satisfactory agreement between the TLS and SfM models in both planimetry (Fig. 9) and altimetry. The topographic profiles generated from both models and for both dates globally match for the ones passing through the crest (C4) and through the C3 gully axis.

This DoD obtained between first February 2016 and 22nd June 2016 can be verified and validated by comparing photographs of some active sectors (Fig. 10), such as:

- The accumulation of blocks and clayey-marly materials at the exit of the G3gully (Fig. 11, A);
- The two rock-topple and debris-fall of dihedrons having affected the C3 & C4 crests (Fig. 10, B–C).

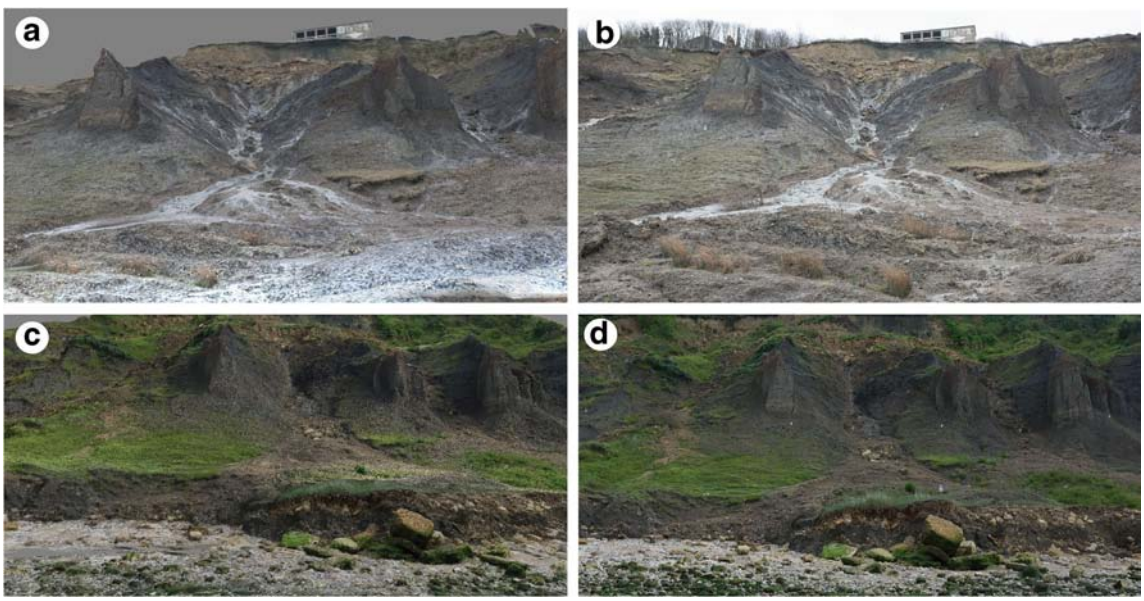

Fig. 8 Textured SfM models: February 2016 (A), June 2016 (C); photograph samples: February 2016 (B), June 2016 (D)

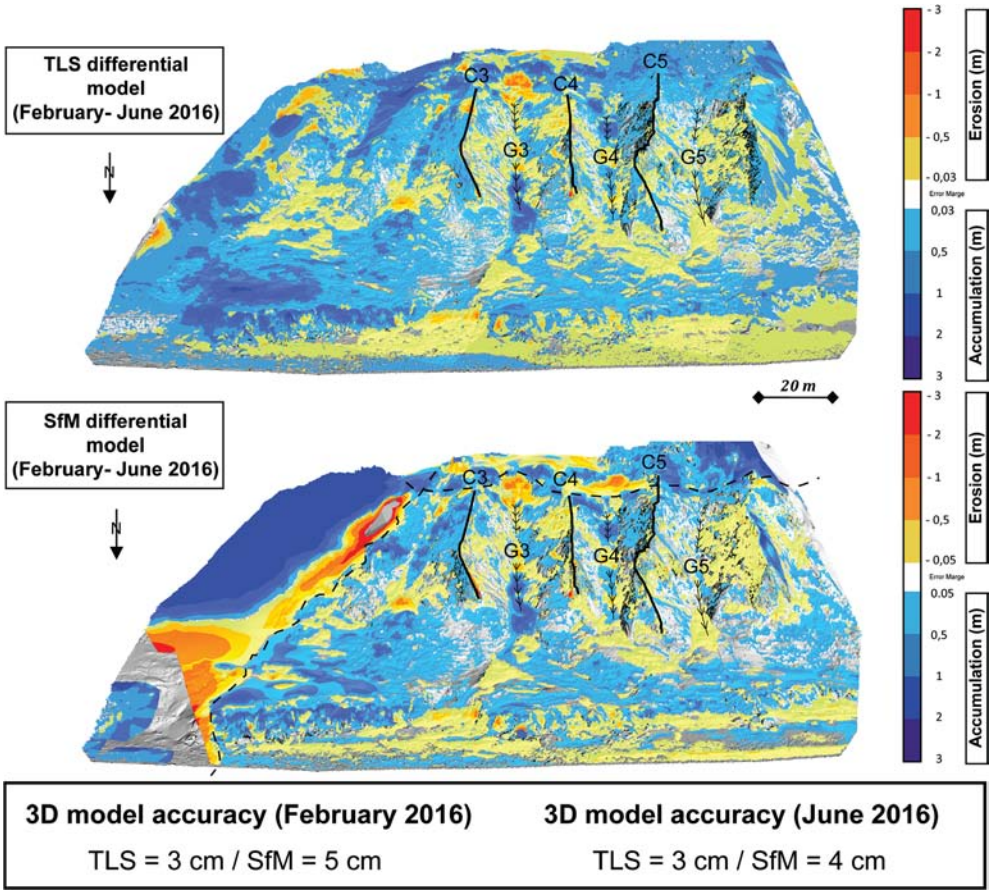

Fig. 9 TLS (a) and SfM (b) difference model—February–June 2016

The SfM differential model between February and June 2016 allows to detect changes for these badlands. It makes clear, and not surprisingly, that (Fig. 10):

- Ablation sectors are located preferentially in the upstream part of the system and on the flanks of the gullies;
- Accumulation sectors are primarily in the downstream part, in the axis of the thalwegs;
- In detail, accumulation and retreat can spatially follow each other in the gullies. Previously, this dynamic-process which was difficult to quantify is now possible thanks to the SfM and TLS methodology;
- The contact of the slope with the sea (basal cliff) also undergoes significant erosion, in spite of strong upstream contribution. This marine erosion seems to be able to explain the retreat of the downstream zone (at the outlets of the gullies) which should have experienced a high accumulation. This reflects the effectiveness of marine actions, and therefore the differences in functioning between badlands systems in continental and marine environments.

The SfM differential models obtained are not sufficiently precise (± 10 cm) to estimate realistic accumulated or eroded volumes. Volumes were therefore calculated on the TLS differential model from manually defined polygons (Fig. 11, A) according to the processes and associated morphologies (ablation zone and accumulation zone).

At this stage, a simple GIS method (Geographical Information System, ArcGis 10.4, Esri) consisting of the delimitation of cubes whose size is derived from the length and width of the reference pixel (5 × 5 cm) and the height expressed by the differential estimated in (z-coordinate). Low erosion/accumulation values below the model margin of error are not taken into account. The volumes obtained by the sum of the cubes for each zone appear realistic (Fig. 11, B).

- The eroded volume estimated at − 18 m³ (± 2 m³) of polygon n°14 on the eastern flank of gully G3 corresponds to localized ablation zones of the order of 7 cm thick on average in a polygon with an area of 260 m². This ablation value is consistent with observations;
- The accumulated volume of + 96 m³ (± 6 m³) of polygon n°13 located in the axis of the gully G3 corresponds fairly well to the ablation volumes of 100 m³ (± 10 m³) of polygons n°14, 16, and 18 located upstream. The materials have thus slipped and were accumulated on the spatial extent of polygon n°13 with an area of 110 m² in the axis of the gully and an average thickness of the order of 90 cm (consistent with observations—Fig. 10, A).

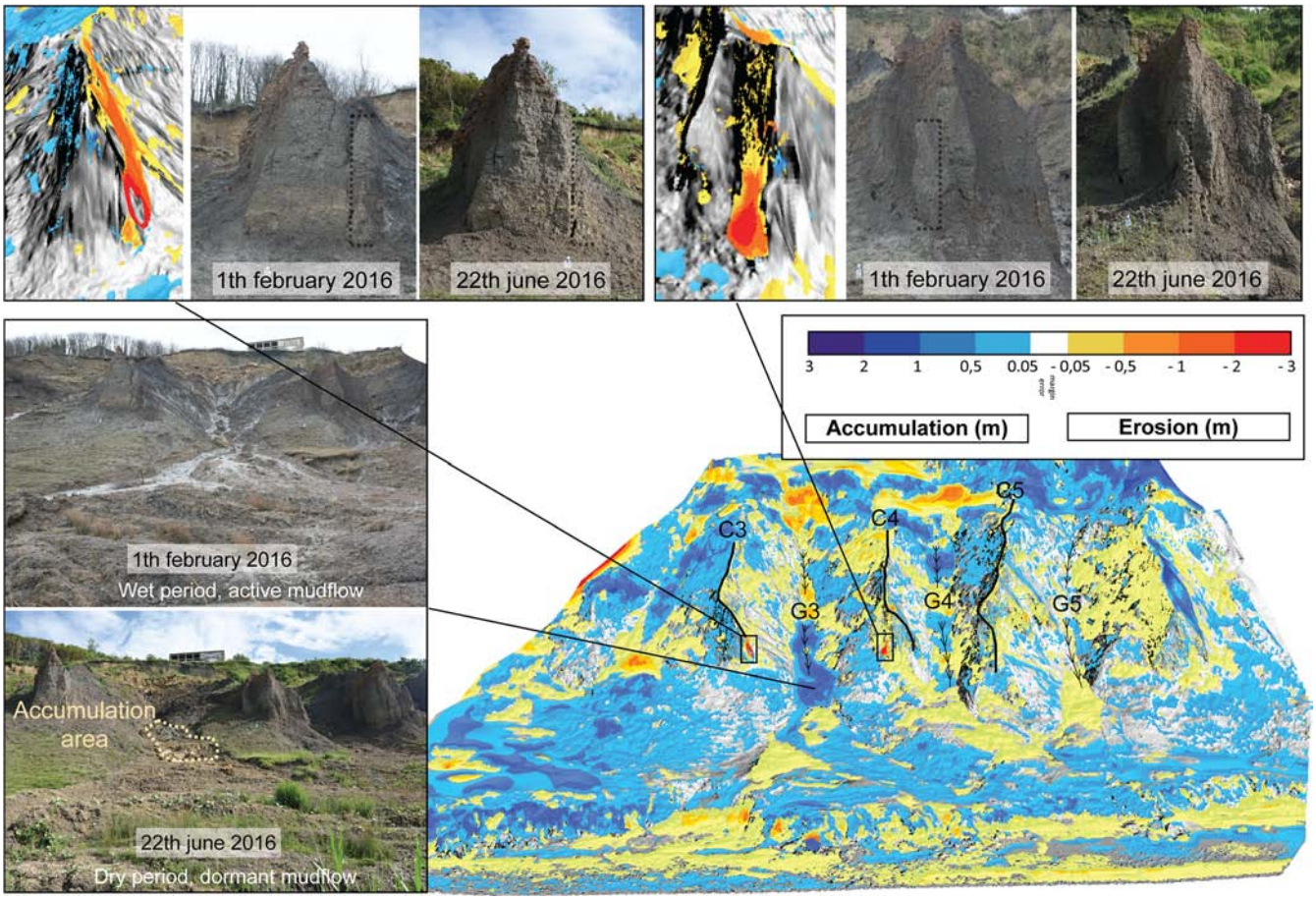

Fig. 10 SfM Difference model between first February 2016 and 22nd June 2016 with photographs of some active sectors for checking and validation of the results

(a)

ID	Action	Minimum Volume (m^3)	Mean Volume (m^3)	Maximum Volume (m^3)	Area (m^2)
13	Accumulation	90	96	103	112
14	Erosion	-16	-18	-20	266
16	Erosion	-32	-35	-39	229
18	Erosion	-43	-47	-51	169
26	Accumulation	56	60	65	104
9	Accumulation	20	22	25	48
5	Accumulation	16	18	21	60
17	Accumulation	12	14	16	47
24	Accumulation	7	8	9	30
11	Accumulation	5	6	7	14
21	Accumulation	4	5	6	13
15	Accumulation	2	3	3	7
3	Accumulation	2	2	3	3
20	Accumulation	1	2	2	5
12	Erosion	-6	-7	-9	48
2	Erosion	-6	-7	-9	38
23	Erosion	-12	-14	-16	80
25	Erosion	-15	-17	-19	124
4	Erosion	-17	-19	-21	229
10	Erosion	-19	-21	-23	133
22	Erosion	-25	-28	-31	240
1	Erosion	-28	-31	-34	109
19	Erosion	-33	-36	-39	292

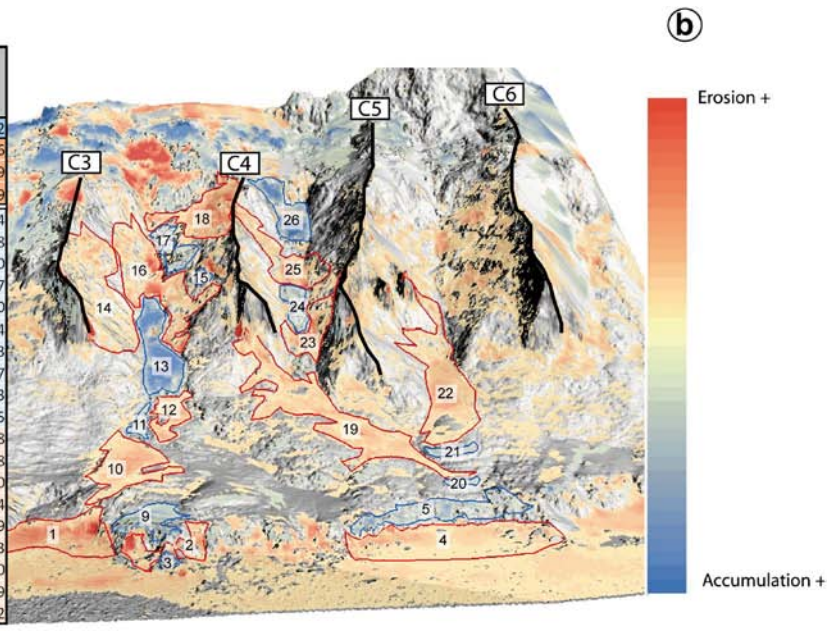

Fig. 11 Estimated volumes (A) and location (B) of the accumulation / erosion zones in the area of interest: TLS February/June 2016

Conclusions

The spatio-temporal high-resolution monitoring protocol of Vaches-Noires cliffs shows the efficiency and complementarity of TLS and SfM methods.

The *terrestrial laser scanner* produces a reference measure that can reach millimeter accuracy. However, the TLS involves a heavy financial investment and also in the field, in the context of coastal modeling, tidal constraints greatly limit the time available for laser scans. The difficulty of multiplying the stations of laser measurements leads to few occlusion zones due to the chaotic topography or vegetation. Even if the methodology is improving (Jaud et al. in press), the equipment associated with the TLS often requires numerous operators in the field (Abellán et al. 2016).

The models derived from the *Structure from Motion* (SfM) method achieve from centimeter to decimeter resolutions, which is a sufficient accuracy for fine monitoring processes. Model comparisons between SfM and TLS confirm the validity of the photogrammetric models with 5 cm of absolute mean error over the area of interest. The quality of the texture, intrinsic to the SfM modeling method, also proves as a powerful tool for analysis and interpretation of three-dimensional landscapes. The implementation of the method in the field is fast and free from the drawback of many operators: this makes it a reactive and cost-effective method in case of major storms, important rainfall events, etc.

Thus, the chosen protocol for monitoring the three gullies (from G3 to G5) allows to densify the number of surveys by giving priority to a monthly SfM survey. These SfM records will still be verified with 2 to 3 annual TLS surveys. In addition, these TLS surveys will allow to assess the accumulated or eroded volumes of the various sectors due to a higher ground resolution of the TLS models. A better monitoring of the evolution of the slope in relation to the meteorological and marine conditions will be possible.

Nevertheless, in the case of chaotic topography, the terrestrial shooting involves problematic discontinuities in the model, which does not allow a homogeneous rendering over the entire study area. To overcome these various obstacles, ways to improve the experimental protocol for the Vaches-Noires site monitoring are under review. Unmanned Aerial Vehicle (UAV) methods at low altitude could overcome the visibility problems induced by land capture (Cawood et al. 2017; Hugenholtz et al. 2013; Tonkin et al. 2014). Experiments have already been carried out, starting from drone or kite, with accuracy close to those obtained by terrestrial photogrammetry (Clapuyt et al. 2016). An ongoing collaboration with the CEREMA (Center for Studies and Expertise on Risks, Environment, Mobility and Development) will shortly be able to compare the SfM terrestrial and drone modeling with the same protocol as the present study based on a TLS reference model.

Manual processing of identification and elimination of vegetation elements will be automated according to guidelines similar to the recent algorithmic developments in this field (Lague et al. 2013; Brodu and Lague 2012). Finally, it will also be necessary to develop an efficient automated method of calculating accumulated/eroded volumes between the different dates.

Acknowledgements

The authors would like to thank Alexandre Thomas for his help during the first SfM acquisition and processing. This research was supported by several projects: the project "Developing Geomorphological mapping skills and datasets in anticipation of subsequent Susceptibility, Vulnerability, Hazard and Risk Mapping" funded by the EUR-OPA European Major Hazards Agreement of the Council of Europe; the ANR project "RICOCHET: multi-RIsk assessment on Coastal territory in a global CHange context" funded by the French Research National Agency (ANR-16-CE03-0008); the Normandy Regional Council via the M2NUM project and the Cerema APHOGEOPHY project.

References

Abellán A, Derron M-H, Jaboyedoff M (2016) "Use of 3D point clouds in geohazards" Special Issue: current challenges and futur trends. Remote Sens 8(2)

Auger P, Mary G (1968) Glissements et coulées boueuses en Basse-Normandie. Rev Géogr Phys Géol Dyn 2:213–224

Bretar F, Arab-Sedze M, Champion J, Pierrot-Deseilligny M, Heggy E, Jacquemoud S (2013) An advanced photogrammetric method to measure surface roughness: application to volcanic terrains in the Piton de la Fournaise, Reunion Island. Remote Sens Environ 135:1–11

Brodu N, Lague D (2012) 3D terrestrial lidar data classification of complex natural scenes using multi-scale dimensionality criterion: applications in geomorphology. ISPRS J Photogramm Remote Sens 68:121–134

Castillo C, Pérez R, James M, Quinton JN, Taguas EV, Gómez JA (2012) Comparing the accuracy of several field methods for measuring gully erosion. Soil Sci Soc Am J 76:1319–1332

Cawood AJ, Bond CE, Howell JA, Butler RWH, Totake Y (2017) LiDAR, UAV or compass-clinometer? Accuracy, coverage and the effects on structural models. J Struct Geol 98:67–82

Chiabrando F, Lingua A, Noardo F, Spano A (2014) 3D modelling of trompe l'oeil decorated vaults using dense matching techniques. ISPRS Annals of the Photogrammetry, Remote Sensing and Spatial Information Sciences II-5:97–104

Clapuyt F, Vanacker V, Van Oost K (2016) Reproducibility of UAV-based earth topography reconstructions based on structure-from-motion algorithms. Geomorphology 260:4–15

Dietrich JT (2016) Riverscape mapping withhelicopter-based structure-from-motion photogrammetry. Geomorphology 252:144–157

Eltner A, Baumgart P (2015) Accuracy constraints of terrestrial Lidar data for soil erosion measurement: application to a Mediterranean field plot. Geomorphology 245(15):243–254

Eltner A, Baumgart P, Maas HG, Faust D (2015) Multi-temporal UAV data for automatic measurement of rill and interrill erosion on loess soil. Earth Surf Process Landf 40:741–755

Eltner A, Kaiser A, Castillo C, Rock G, Neugirg F, Abellán A (2016) Image-based surface reconstruction in geomorphometry—merits, limits and developments. Earth Surface Dynamics 4:359–389

Favalli M, Fornaciai A, Isola I, Tarquini S, Nannipieri L (2012) Multiview 3D reconstruction in geosciences. Comput Geosci 44:168–176

Harwin S, Lucieer A (2012) Assessing the accuracy of georeferenced point clouds produced via multi-view stereopsis from unmanned aerial vehicle (UAV) imagery. Remote Sens 4(6):1573–1599

Hugenholtz CH, Whitehead K, Brown OW, Barchyn TE, Moorman BJ, LeClaire A, Riddell K, Hamilton T (2013) Geomorphological mapping with a small unmanned aircraft system (sUAS): feature detection and accuracy assessment of a photogrammetrically-derived digital terrain model. Geomorphology 194:16–24

Immerzeel WW, Kraaijenbrink A, Shea JM, Shrestha AB, Pellicciotti F, Bierkens MFP, De Jong SM (2014) High resolution monitoring of Himalayan glacier dynamics using unmanned aerial vehicles. Remote Sens Environ 150:93–103

Jaboyedoff M, Oppikofer T, Abellán A, Derron M-H, Loye A, Metzger R, Pedrazzini A (2012) Use of LIDAR in landslide investigations : a review. *Natural Hazards*, pp:5–28

James MR, Quinton JN (2014) Ultra-rapid topographic surveying for complex environments: the hand-held mobile laser scanner (HMLS). Earth Surf Process Landf 39(1):138–142

James MR, Robson S (2012) Straightforward reconstruction of 3D surfaces and topography with a camera: accuracy and geoscience application. *Journal of Geophysical Research*, vol 117

James MR, Robson S (2014) Mitigating systematic error in topographic models derived from UAV and ground-based image networks. Earth Surf Process Landf 39:1413–1420

Jaud M, Letortu P, Augereau E, Le Dantec N, Beauverger M, Cuq V., Prunier C, Le Bivic R, Delacourt C (in press) Pseudo-direct georeferencing of terrestrial laser scanning data for coastal landscape surveying. Eur J Remote Sens

Kaiser A, Neugirg F, Rock G, Müller C, Haas F, Ries J, Schmidt J (2014) Small-scale surface reconstruction and volume calculation of soil erosion in complex moroccan gully morphology using structure-from-motion. Remote Sens 6:7050–7080

Lague D, Brodu N, Leroux J (2013) Accurate 3D comparison of complex topography with terrestrial laser scanner: application to the Rangitikei canyon (N-Z). ISPRS J Photogramm Remote Sens 82:10–26

Letortu P, Costa S, Maquaire O, Delacourt C, Augereau E, Davidson R, Suanez S, Nabucet J (2015) Retreat rates, modalities and agents responsible for erosion along the coastal chalk cliffs of Upper Normandy: the contribution of terrestrial laser scanning. Geomorphology 245:3–14

Lowe, D. (1999) 'Object recognition from local scale-invariant features', *Proceedings of the International Conference of Computer Vision*, Corfu, Greece

Lowe D (2004) Distinctive image features from scale-invariant keypoints. Int J Comput Vis 60:91–110

Lucieer A, De Jong S, Turner D (2013) Mapping landslide displacements using structure from motion (SfM) and image correlation of multi-temporal UAV photography. Prog Phys Geogr 38:1–20

Mancini F, Dubbini M, Gattelli M, Stecchi F, Fabbri S, Gabbianelli G (2013) Using unmanned aerial vehicles (UAV) for high-resolution reconstruction of topography: the structure-from-motion approach on coastal environments. Remote Sens 5:6880–6898

Maquaire O, Malet JP (2006) Shallow landsliding., In: Boardman J, Poesen, J (eds) Soil erosion in Europe. Willy

Maquaire O, Afchain P, Launay A, Costa S, Lissak C, Fressard M, Letortu P, Davidson R, Thiery Y (2013) Evolution à long terme des falaises des 'Vaches Noires' et occurence des glissements (Calvados, Basse-Normandie, France). *Recueil des actes des Journées 'Aléas Gravitaire', Grenoble, 17–18 septembre*

Michelletti N, Chandler JH, Lane SN (2015) Investigating the geomorphological potential of freely available and accessible structure-from-motion photogrammetry using a smartphone. Earth Surf Process Landf 40:473–486

Nolan M, Larsen C, Sturm M (2015) Mapping snow depth from manned aircraft on landscape scales at centimeter resolution using structure-from-motion photogrammetry. Cryosphere 9:1445–1463

Nouwakpo SK, Weltz MA, McGuire K (2015) Assessing the performance of structure-from-motion photogrammetry and terrestrial lidar for reconstructing soil surface microtopography of naturally vegetated plots. Earth Surf Process Landf 41:308–322

Piermattei L, Carturan L, De Blasi F, Tarolli P, Dalla Fontana G, Vettore A, Pfeifer N (2016) Suitability of ground based SfM-MVS for monitoring glacial and periglacial processes. Earth Surface Dynamics 4:425–443

Prokop A, Panholzer H (2009) Assessing the capability of terrestrial laser scanning for monitoring slow moving landslides. Nat Hazards Earth Syst Sci 9:1924–1928

Prosdocimi M, Calligaro S, Sofia G, Dalla Fontana G, Tarolli P (2015) Bank erosion in agricultural drainage networks: new challenges from structure-from-motion photogrammetry for post-event analysis. Earth Surf Process Landf 40:1891–1906

Rippin DM, Pomfret A, King N (2015) High resolution mapping of supraglacial drainage pathways reveals link between micro-channel drainage density, surface roughness and surface reflectance. Earth Surf Process Landf 40:1279–1290

Roer I, Nyenhuis M (2007) Rockglacier activity studies on a regional scale: comparison of geomorphological mapping and photogrammetric monitoring. Earth Surf Process Landf 32:1747–1758

Ruggles S, Clark J, Franke KW, Wolfe D, Reimschiissel B, Martin RA, Okeson TJ, Hedengren JD (2016) Comparison of SfM computer vision point clouds of a landslide derived from multiple small UAV platforms and sensors to a TLS based model. Journal of Unmanned Vehicule Systems 4:246–265

Ružić I, Marovic I, Benac C, Ilic S (2014) Coastal cliff geometry derived from structure-from-motion photogrammetry at Stara Baka, Krk Island, Croatia. Geo-Mar Lett 34:555–565

Schürch PL, Densmore AJ, Rosser N, Lim MW, McArdell B (2011) Detection of surface change in complex topography using terrestrial laser scanning: application to the Illgraben debris-flow channel. Earth Surf Process Landf 36(14):1847–1859

Shan J, Toth CK (2008) Topographic laser ranging and scanning: principles and processing. CRC Press, Taylor & Francis

Slatcher N, James MR, Calvari S, Ganci G, Browning J (2015) Quantifying effusion rates at active volcanoes through integrated time-lapse laser scanning and photography. Remote Sens 7:14967–14987

Smith MW, Vericat D (2015) From experimental plots to experimental landscapes: topography, erosion and deposition in sub-humid badlands from structure-from-motion photogrammetry. Earth Surf Process Landf 40:1656–1671

Smith MW, Carrivick JL, Quincey DJ (2015) Structure from motion photogrammetry in physical geography. Prog Phys Geogr

Sofia G, Hillier JK, Conway SJ (2016) Frontiers in geomorphometry and earth surface dynamics: possibilities, limitations and perspectives. Earth Surface Dynamics 4:1–5

Stöcker C, Eltner A, Karrash P (2015) Measuring gullies by synergetic application of UAV and close range photogrammetry – a case study from Andalusia, Spain. Catena 132:1–11

Stumpf A, Malet JP, Allemand P, Pierrot-Deseilligny M, Skupinski G (2014) Ground-based multi-view photogrammetry for the monitoring of landslide deformation and erosion. Geomorphology 231:130–145

Tahar KN (2013) An evaluation on different number of ground control points in unmanned aerial vehicle photogrammetric block. *ISPRS 8th 3DGeoInfo Conference & WG II/2 Workshop, Istanbul, Turkey*, p 93–98

Teza G, Galgaro A, Zaltron N, Genevois R (2007) Terrestrial laser scanner to detect landslide displacement fields: a new approach. Int J Remote Sens 28:3425–3446

Tonkin TN, Midgley NG, Graham DJ, Labadz JC (2014) The potential of small unmanned aircraft systems and structure-from-motion for topographic surveys: a test of emerging integrated approaches at cwm Idwal, North Wales. Geomorphology 226:35–43

Tournadre V, Pierrot-Deseilligny M, Faure PH (2015) UAV linear photogrammetry. The International Archives of the Photogrammetry, Remote Sensing and Spatial Information Sciences, vol. XL-3/W3, p 327–333

Travelletti J, Malet JP, Samyn K, Grandjean G, Jaboyedoff M (2013) Control of landslide retrogression by discontinuities: evidence by the integration of airborn- and ground-based geophysical information. Landslides 10:37–54

Westoby MJ, Brasington J, Glasser NF, Hambrey MJ, Reynolds JM (2012) "structure-from-motion" photogrammetry: a low cost, effective tool for geoscience applications. Geomorphology 179:300–314

Wheaton JM, Brasington J, Darby SE (2009) Accounting for uncertainty in DEMs from repeat topographic surveys: improved sediment budgets. Earth Surf Process Landf 35(2):136–156

Woodget A, Carbonneau P, Visser F, Maddock I (2015) Quantifying submerged fluvial topography using hyperspatial resolution UAS imagery and structure from motion photogrammetry. Earth Surf Process Landf 40:47–64

M. Medjkane (✉) · O. Maquaire · S. Costa · T. Roulland · . Davidson
Normandie Univ, Unicaen, CNRS, LETG-Caen,
14000, Caen, France
Email: mohand.medjkane@unicaen.fr

P. Letortu
Laboratory LETG-Brest Géomer, IUEM,
University of Bretagne Occidentale,
Rue Dumont d'Urville, 29280, Plouzané, France

C. Fauchard · R. Antoine
CEREMA Normandie-Centre,
Rouen, France